Epoxidation of Acyclic Chiral Allylic Alcohols with Peroxy Acids: Spiro or Planar Butterfly Transition Structures? A Computational DFT Answer

Mauro Freccero,[†] Remo Gandolfi,[†] Mirko Sarzi-Amadè,*[,†] and Augusto Rastelli[‡]

Dipartimento di Chimica Organica, Università di Pavia, V.le Taramelli 10, 27100, Pavia, Italy, and Dipartimento di Chimica, Università di Modena, Via Campi 183, 41100, Modena, Italy

Received September 29, 1999

The mechanism of the epoxidation of two chiral allylic alcohols, i.e., 3-methyl-3-buten-2-ol and (*Z*)-3-penten-2-ol, with peroxyformic acid has been investigated by locating 20 transition structures with the B3LYP/6-31G* method and by evaluating their electronic energy also at the B3LYP/6-311+G**//B3LYP/6-31G* theory level. Relative stability of TSs, as far as electronic energy is concerned, is basis set dependent; moreover, it also depends on entropy and solvent effects. Free enthalpies, calculated by using electronic energy at the higher theory level and with inclusion of solvent effects, indicates that syn,exo TSs, where the olefinic OH group hydrogen bonds the peroxy oxygens of the peroxy acid, outweigh syn,endo TSs, where the peroxy acid carbonyl oxygen is involved in hydrogen bonding. In the former TSs the peroxy acid moiety maintains its planar geometry while in the latter ones a strong out-of-plane distortion of peroxy acid is observed. This distortion makes it viable an unprecedented 1,2-H shift, as a possible alternative to the 1,4-H shift, for the peroxy acid hydrogen. In fact, for one syn,endo TS IRC analysis demonstrated that the 1,2-H shift mechanism is actually operative. *The geometry of all TSs substantially conforms to a spiro (i.e., with the peroxy acid plane almost perpendicular to the C═C bond axis) butterfly orientation of the reactants while no TS resembles, even loosely, the planar butterfly structure.* Theoretical threo/erythro epoxide ratios are in fair accord with experimental data. Calculations indicate that threo epoxides derive mostly from TSs in which the olefinic OH assumes an outside conformation while erythro epoxides originate from TSs with the OH group in an inside position. Computational findings do not support the qualitative TS models recently proposed for these reactions.

In 1950, Bartlett proposed the "butterfly" mechanism (**A**, Figure 1), with concerted formation of the new oxirane bonds, for oxygen transfer in the epoxidation reaction of olefins with peroxy acids.[1] Only recently, Bach et al.[2] and Houk et al.[3] definitely demonstrated, by high-level calculations, that the reaction of peroxyformic acid with ethylene goes via a concerted synchronous transition structure (TS) (**B**, Figure 1) while concerted asynchronous TSs were located for substituted olefins. A distinctive feature of all these TSs is that the peroxy acid plane is exactly perpendicular (e.g., in the reaction with ethylene) or almost perpendicular to the C═C bond axis. That is, all TSs have a spiro structure while no first-order saddle point with planar geometry (in which the C═C bond axis lies in the peroxy acid plane) could be located, and this reactant orientation was estimated to be ∼4−5 kcal/mol higher in energy than its spiro counterpart.[3b,4] It is quite evident that this finding is due to the intrinsically higher stability of the tetrahedral-like array of atoms around the transferred oxygen in the spiro TS as compared to the square-planar like arrangement present in the planar TS. It remains to be established whether the peroxy acid can adopt a concerted planar butterfly approach to C═C in the reaction of olefins for which spiro orientation is impeded by insurmountable steric interactions (such as in anti sesquinorbornene).[4]

Actually, there is much less consensus about the epoxidation mechanism of allylic alcohols, and several features are still in dispute. In particular, in these systems the tendency to maximize hydrogen bonding might, in concurrence with steric effects in the case of heavily substituted derivatives, even force the reacting system to choose the inherently less stable planar transition structure.

In the 1950s, researchers soon realized that facial selectivity in epoxidation reactions can be efficiently driven by interaction between an allylic OH group and the peroxy acid: for example, the syn epoxide is largely prevalent over the anti isomer (syn/anti = 95:5 in CH_2Cl_2 at 0 °C)[5,6] in the reaction of *m*-CPBA with 2-cyclohexen-1-ol. This syn directing effect was implemented by Henbest (in 1959) in the Bartlett mechanism by suggesting a hydrogen-bonding interaction between the OH group and the distal peroxy oxygen of the peroxy acid in a transition structure with a planar butterfly geometry (see **C** in Figure 1).[5] Several years later, this planar model was still considered more reasonable than its spiro

* To whom correspondence should be addressed. Phone: +39 382 507668. Fax: +39 382 507323. E-mail: nmr@chifis.unipv.it.
[†] Università diPavia.
[‡] Università di Modena.

(1) Bartlett, P. D. *Rec. Chem. Prog. II* **1950**, 47.
(2) (a) Bach, R. D.; Glukhovtsev, M. N.; Gonzales, C.; Marquez, M.; Estevez, C. M.; Baboul, A. G.; Schlegel, H. B. *J. Phys. Chem. A* **1997**, *101*, 6092. (b) Bach, R. D.; Glukhovtsev, M. N.; Gonzales, C. *J. Am. Chem. Soc.* **1998**, *120*, 9902.
(3) (a) Singleton, D. A.; Merrigan, S. R.; Liu, J.; Houk, K. N. *J. Am. Chem. Soc.* **1997**, *119*, 3385. (b) Houk, K. N.; Liu, J.; DeMello, N. C.; Condroski, K. R. *J. Am. Chem. Soc.* **1997**, *119*, 10147.
(4) (a) Koener, T.; Slebocka-Tilk, H.; Brown R. S. *J. Org. Chem.* **1999**, *64*, 196. (b) Rebek, J., Jr.; Marshall, L.; McManis, J.; Wolak, R. *J. Org. Chem.* **1986**, *51*, 1649.
(5) Henbest, H. B.; Wilson, R. A. L. *J. Chem. Soc.* **1959**, 1958.
(6) Itoh, T.; Jitsukawa, K.; Kaneda, K.; Teranishi, S. *J. Am. Chem. Soc.* **1979**, *101*, 159.

10.1021/jo991530k CCC: $19.00
Published on Web 03/15/2000

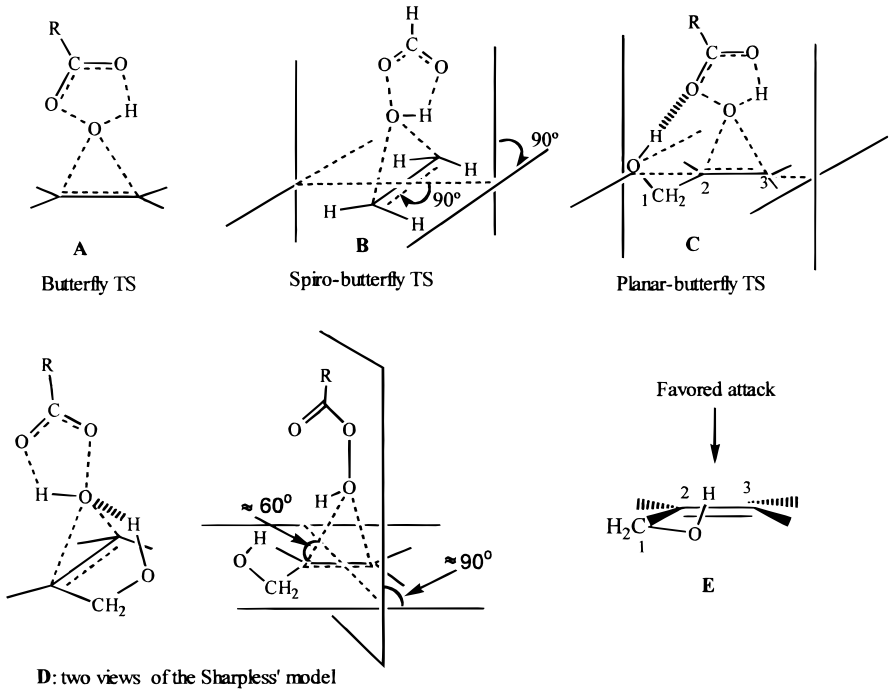

Figure 1. Schematic description of transition structures for peroxy acid epoxidation of olefin [**A** (Bartlett), **B** (Bach, Houk)] and allylic alcohols [**C** (Hembest), **D** (Sharpless), **E** (Pierre)].

counterpart by Whitham et al. (1970).[7] Other authors seem to have adhered to the Henbest model even if the spiro vs planar problem was not clearly discussed by them.[6,8] A more detailed (even if qualitative) transition structure (for both cyclic and acyclic allylic alcohols) was advanced by Sharpless in 1979 (i.e., **D**).[9a] This model differs from that of Henbest because (i) it is a spiro TS with the peroxy acid plane oriented at 60° with respect to the C=C bond axis and perpendicular to the alkene plane and (ii) hydrogen bonding involves the proximal peroxy oxygen and not the distal one. This model gained wide acceptance by organic chemists[10,11] even if mixed models, namely spiro TS with hydrogen bonding involving the distal peroxy oxygen, were also considered.[12] Moreover, recently the planar TS with hydrogen bonding at distal peroxy oxygen was adopted by Adam et al. in order to explain the diastereoselectivity of the *m*-CPBA epoxidations of acyclic chiral allylic alcohols (see below).[13a−g] This model was also used for epoxidations with both organo sulfonic peracids[14] and hydroperoxyphosphinic acid.[15]

It is useful to emphasize that, in all the models described above, the OH group adopts an "outside" conformation (an optimal value of ∼120° for the $O-C_1-C_2-C_3$ angle was suggested by Sharpless[9] and by Adam)[13a−g] and hydrogen bonds the peroxy oxygens (not the carbonyl oxygen) of the peroxy acid. As for the OH conformation, Pierre et al. argued that, in the case of acyclic alcohols, TSs with the OH group in an "inside" position (**E**, the $O-C_1-C_2-C_3 \approx 0°$) are reasonable models to explain the stereochemical outcome of epoxidations.[16]

This was the state of affairs when very recently (1998) Bach et al., on the basis of B3LYP/6-311G** calculations on the reaction of propenol with peroxyformic acid (PFA), *raised the possibility that (at odds with previous TS models proposed by experimentalists) the most favored hydrogen-bonding interaction actually involves not the peroxy oxygens but the carbonyl oxygen* of the peroxy-acid.[17] They located two TSs with the OH group either in an inside (more favored) or outside conformation. We have successively complemented this result, with calculations of the same type, by demonstrating that in the reaction of propenol with PFA actually at least four syn TSs (out of the five syn TSs where hydrogen bonding is operative) compete each other (see Figure 2): the two syn,endo TSs located by Bach (*syn,endo*-**1a** and *syn,endo*-

(7) Chamberlain, P.; Roberts, M. L.; Whitham, G. H. *J. Chem. Soc. B* **1970**, 1374.
(8) Johnson, M. R.; Kishi, Y. *Tetrahedron Lett.* **1979**, 4347.
(9) (a) Sharpless, K. B.; Verhoeven, T. R. *Aldrichimica Acta* **1979**, *12*, 63. (b) Sharpless, K. B.; Rossiter, B. E.; Verhoeven T. R. *Tetrahedron Lett.* **1979**, 4733.
(10) Kocovsky, P.; Stary, I. *J. Org. Chem.* **1990**, *55*, 3236.
(11) Hoveyda, A. H.; Evans, D. A.; Fu, G. C. *Chem. Rev.* **1993**, *93*, 1307.
(12) Narula, A. S. *Tetrahedron Lett.* **1983**, *24*, 5421.
(13) (a) Adam, W.; Nestler, B. *Tetrahedron Lett.* **1993**, *34*, 611. (b) Adam, W.; Smerz, A. K. *J. Org. Chem.* **1996**, *61*, 3506. (c) Adam, W.; Kumar, R.; Reddy, I.; Renz, M. *Angew. Chem., Int. Ed. Engl.* **1996**, *35*, 880. (d) Adam, W.; Corma, A.; Reddy, I.; Renz, M. *J. Org. Chem.* **1997**, *62*, 3631. (e) Adam, W.; Stegmann, V. R.; Saha-Moller, C. R. *J. Am. Chem. Soc.* **1999**, *121*, 1879. (f) Adam, W.; Mitchell, C. M.; Saha-Moller, C. R. *J. Org. Chem.* **1999**, *64*, 3699. (g) Adam, W.; Degen, H. G.; Saha-Moller, C. R. *J. Org. Chem.* **1999**, *64*, 1274. (h) Adam, W.; Prechtl, F.; Richter, M. J.; Smerz, A. K. *Tetrahedron Lett.* **1993**, *34*, 8427. (i) Adam, W.; Smerz, A. K *Tetrahedron* **1995**, *51*, 13039. (j) Adam, W.; Brunker, H.; Kumar, A. S.; Peters, E. A.; Peters, K.; Schneider, U.; von Schnering, H. G. *J. Am. Chem. Soc.* **1996**, *118*, 1899. (k) Adam, W.; Paredes, R.; Smerz, A. K.; Veloza, A. L. *Liebigs Ann./Recl.* **1997**, 547. (l) Adam, W.; Paredes, R.; Smerz, A. K.; Veloza, A. *Eur. J. Org. Chem.* **1998**, 349. (m) Adam, W.; Mitchell, C. M.; Saha-Moller, C. R. *Eur. J. Org. Chem.* **1999**, 785. (n) Note added in proof: in a recent review (Adam, W.; Wirth, T. *Acc. Chem. Res.* **1999**, *32*, 703) Adam et al., while maintaining a "planar" geometry for peroxy acid epoxidation TSs, adopt a "Bach" model for hydrogen bonding; i.e., they now prefer hydrogen bond to peroxy acid carbonyl oxygen.
(14) Kluge, R.; Schulz, M.; Liebsch, S. *Tetrahedron* **1996**, *52*, 2957.
(15) Kende, A. S.; Delair, P.; Blass, B. E. *Tetrahedron Lett.* **1994**, *35*, 8123.
(16) Chautemps, P.; Pierre, J. L. *Tetrahedron* **1976**, *32*, 549.
(17) Bach, R. D.; Estévez, C. M.; Winter J. E.; Glukhovtsev, M. N. *J. Am. Chem. Soc.* **1998**, *120*, 680.

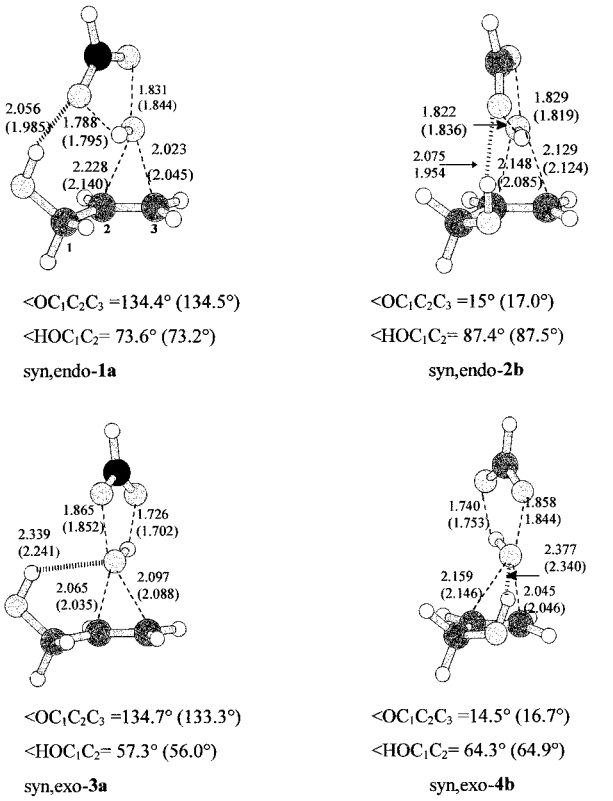

Figure 2. B3LYP-optimized transition structures (bond lengths in Å) for epoxidation of 2-propen-1-ol at the B3LYP/6-311+G** (B3LYP/6-31G*) level.

2b) and two further TSs with syn,exo orientation (*syn*-,*exo*-**3a** and *syn*,*exo*-**4b**).[18] In the latter TSs, the OH group hydrogen bonds the peroxy oxygens (as in the models proposed by experimentalists) and adopts either an outside (in **3a**) or inside (in **4b**) conformation.

One must be careful in drawing definitive conclusions about the relative energies of these four syn TSs because they depend both on the calculation level and on the solvent effect. The highest level calculation used by us [B3LYP/6-311+G** with introduction of electrostatic solvent (CH_2Cl_2) effects by the Tomasi model] indicates the following stability order: *syn*,*exo*-**4b** ≈ *syn*,*exo*-**3a** > *syn*,*endo*-**2b** > *syn*,*endo*-**1a** ($G^{\ddagger}_{rel,sol\ (CH_2Cl_2)}$ = 0.00, 0.30, 1.86, and 2.34 kcal/mol). This order looks somewhat different from that based on B3LYP/6-31G* electronic energies, that is: *syn*,*endo*-**2b** > *syn*,*exo*-**4b** > *syn*,*exo*-**3a** > *syn*,*endo*-**1a** ($E^{\ddagger}_{rel}$ = 0.00, 1.77, 2.03, and 2.12 kcal/mol) (see also the Computational Methods).

It is important to stress that TS geometries **1a**−**4b** obtained by the B3LYP/6-31G* method are very similar to those deriving from B3LYP/6-311+G** calculations, and in particular, in all TSs of Figure 2 the reactants show a spiro butterfly orientation. Thus, our results suggest that geometries do not greatly depend on the calculation level. The only not negligible difference is a small lengthening of the H-bond distances (slightly longer at the higher level by 0.03−0.12 Å) in all TSs but it does not significantly influence the TS relative energies (Table 1).

At this point, several intriguing questions seek answers: Can the spiro transition structure be safely considered favored over the planar one also for TSs of the reactions involving sterically congested chiral acyclic allylic alcohols? What is the relative role of TSs with OH in the inside and outside conformation in determining the stereochemical outcome for the reactions of these derivatives? Do TSs with hydrogen bonding to carbonyl oxygen actually compete with TSs with hydrogen bonding to peroxy oxygens?

These questions were explicitly (the first one) or implicitly addressed by Adam et al. in the discussion of diastereoselectivity (threo/erythro ratio) of the epoxidation of chiral acyclic alcohols with allylic strain (see Scheme 1).[13a−g] These derivatives were used by several authors but in particular by Adam et al. in a systematic study of the mechanism of epoxidation reactions. Chiral allylic alcohols were considered "useful mechanistic probes for the investigation of transition structures...to obtain valuable information on the geometry of the oxygen transfer process in epoxidation reactions"[13e] with peroxy acids, dioxiranes, ketone perhydrates, as well as epoxidation catalyzed by metal complexes.[13]

Models proposed (1993−1999) by Adam et al. to rationalize the observed threo-erythro selectivity ("stereochemical fingerprint for transition-state structures")[13e] are very simple and appealing ones. In the case of the reactions of peroxy acids with methyl substituted chiral allylic alcohols, it is assumed that (i) the only relevant reaction channels are those that feature hydrogen-bonding interactions in the TS (i.e., only syn TSs have been considered); (ii) only two planar butterfly TSs[13g] [exemplified by *threo*-**11** and *erythro*-**12** (Scheme 1), which are TS models for the epoxidation of **6**] compete each other to determine the diastereoselectivity of the reaction; (iii) hydrogen bonding involves only the distal peroxy oxygen[13n] and imposes the conformational choice to the MeCHOH− moiety (with the $O-C_2-C_3-C_4$ dihedral angle very close to 120°, that is, OH must occupies an "outside" position); and (iv) the relative stability of threo as compared to erythro TSs is substantially determined by ^{1,2}A and ^{1,3}A strains.

No theoretical investigation is available to date for peroxy acid epoxidation of acyclic allylic alcohols with ^{1,2}A and ^{1,3}A strains. Given the importance of the studies with the chiral acyclic allylic alcohols of Scheme 1, there is an obvious high interest in verifying by calculations these qualitative models, which seem so efficient in explaining the experimental results. Thus, we performed DFT studies on the peroxyformic acid epoxidation of the most representative chiral allylic alcohols of Scheme 1: the 3-methyl-3-buten-2-ol (i.e., **5**) and the (Z)-3-penten-2-ol (i.e., **6**). Compound **5** is the only derivative for which the erythro attack is dominant while **6** exhibits one of the highest threo selectivities (Scheme 1).

The aim of our study was to reliably address the points still open in the mechanism of acyclic allylic alcohols epoxidation with special emphasis on the spiro/planar geometry problem. We were also interested in defining to what extent good DFT calculations, which seem to perform so well for so many problems, can reproduce the facial selectivity[19,20] of epoxidation of chiral acyclic allylic alcohols.

(18) Freccero, M.; Gandolfi, R.; Sarzi-Amadè, M.; Rastelli, A. *J. Org. Chem.* **1999**, *64*, 3853.

(19) For previous PM3 and B3LYP studies, respectively, on facial selectivity of cyclic alkenes see ref 20a and 20b.

(20) (a) Lucero, M.; Houk, K. N. *J. Org. Chem.* **1998**, *63*, 6973. (b) Freccero, M.; Gandolfi, R.; Sarzi-Amadè, M. *Tetrahedron* **1999**, *55*, 11309.

Table 1. Relative B3LYP Electronic Energies for TSs of the PFA Epoxidation of 2-Propen-1-ol Calculated with Different Basis Sets[a,b]

TS	6-31G*	6-31+G*	6-311G**	6-311+G**	//6-31+G*	//6-311G**	//6-311+G**	//cc-pVTZ	//AUG-cc-pVTZ
1a	2.12	1.32	2.15	1.39	1.37	2.18	1.47	1.69	1.39
2b	0.00	0.00	0.00	0.00	0.00	0.00	0.00	0.00	0.00
3a	2.03	0.25	1.67	0.39	0.21	1.66	0.36	1.34	0.83
4b	1.77	0.20	1.16	0.19	0.20	1.17	0.17	0.92	0.62
anti,endo	6.54	4.40	6.25	4.38	4.42	6.24	4.35		
anti,exo	6.02	3.65	5.57	3.65	3.61	5.56	3.55		

[a] Columns 2−5 report values for fully optimized structures while columns 6−10 report values for single-point calculations on the B3LYP/6-31G* geometry. [b] B3LYP electronic energies for fully optimized **2b** with different basis sets (in parentheses are values from single-point calculations on the B3LYP/6-31G* geometry) are as follows: 6-31G* = −457.978212; 6-31+G* = −458.002342 (−458.002070); 6-311G** = −458.124987 (−458.124700); 6-311+G** = −458.138419 (−458.137893). Electronic energies for **2b** from single-point calculations on the B3LYP/6-31G*-optimized geometry with cc-pVTZ and AUG-cc-pVTZ basis sets: −458.172495 and −458.180812, respectively.

Scheme 1

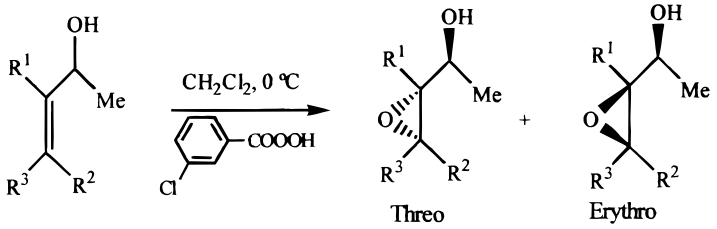

Olefin	R^1	R^2	R^3	epoxide	Threo	epoxide	Erythro
5	Me	H	H	**7**	45%	**8**	55%
6	H	Me	H	**9**	95%	**10**	5%
	H	Me	Me		95%		5%
	Me	Me	H		90%		10%
	H	H	H		60%		40%
	H	H	Me		64%		36%
	Me	H	Me		48%		52%

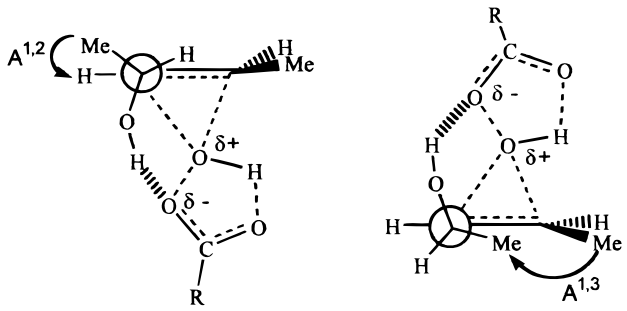

11 (Threo TS) **12** (Erythro TS)

Adam's TS models

Computational Methods

The B3LYP hybrid functional, consisting of the nonlocal exchange functional of Becke's three-parameter set and the nonlocal correlation function of Lee, Yang, and Parr, with the 6-31G* basis set was used.[21,22] This method, which includes both dynamic and nondynamic electron correlation, is now well established as a method that can describe, reliably enough, potential energy surfaces for epoxidation reactions with peroxy acids and dioxiranes.[2,3,23] Basis set extensions with polarization function also for hydrogen (i.e., B3LYP/6-311G**) as well as introduction of diffuse functions (i.e., B3LYP/6-311+G**) are certainly useful to more properly describe lone pairs[24] and hydrogen-bonding interactions.[25] The usual dilemma between financial ruin and low-level calculations can be satisfactorily solved for the systems under study by carrying out geometry optimization at the B3LYP/6-31G* level and improving the energy description by single point calculations with more extended basis sets. In fact, we could show (by studying the reaction of propenol with peroxyformic acid)[18] that optimized TS geometries do not heavily change on going from B3LYP/6-31G* to B3LYP/6-311+G** (see Figure 2) via B3LYP/6-311G** and B3LYP/6-31+G methods. However, not only absolute but also the relative TS energies can change appreciably. In particular, a significant variation in relative

(21) Becke, A. D. *J. Chem. Phys.* **1993**, *98*, 1372.
(22) Lee, C.; Yang, W.; Parr, R. G. *Phys. Rev. B* **1988**, *37*, 785.
(23) (a) Freccero, M.; Gandolfi, R.; Sarzi-Amadè, M.; Rastelli, R. *Tetrahedron* **1998**, *54*, 6123. (b) Freccero, M.; Gandolfi, R.; Sarzi-Amadè, M.; Rastelli, A. *Tetrahedron* **1998**, *54*, 12323.
(24) Castejon, H.; Wiberg, K. B. *J. Am. Chem. Soc.* **1999**, *121*, 2139.
(25) Pan, Y.; McAllister, M. A. *J. Am. Chem. Soc.* **1998**, *120*, 166.

Table 2. Relative Free Enthalpies (G_{rel}), Bond Lengths (Å), Angles (Deg), OH Stretching Frequencies (ν_{OH}), and Dipole Moments (μ) of 3-Methyl-3-buten-2-ol (5a−d) and (*Z*)-3-Penten-2-ol (6a−d) Conformers at the B3LYP/6-31G* Level

conformer	G_{rel} (kcal/mol)	C_3-C_4	HOC_2C_3	$OC_2C_3C_4$	ν_{OH} (cm^{-1})	μ (Debye)
5a	0.00	1.337	56.8	−118.3	3733	1.13
5b	0.91	1.336	−64.9	−2.7	3717	1.71
5c	0.85	1.337	−61.9	120.1	3716	1.22
5d	0.07	1.337	53.1	16.4	3731	1.59
6a	0.00	1.339	52.5	−123.7	3736	1.86
6b	1.01	1.340	−46.3	−48.1	3725	1.40
6c	4.25	1.340	−58.7	132.2	3720	1.78
6d	1.51	1.340	50.8	29.07	3735	1.31

energies takes place (Table 1) when the diffuse function is introduced (i.e., on going from B3LYP/6-31G* to B3LYP/6-31+G* theory level as well as from B3LYP/6-311G** to B3LYP/6-311+G** method) while relatively minor changes are observed on passing from B3LYP/6-31G* to B3LYP/6-311G**. Fortunately, probably as a result of the remarkable geometry constancy when basis set is changed, higher level single-point calculations on B3LYP/6-31G*-optimized geometries very closely reproduce the relative energies obtained by the corresponding higher level full optimization procedures as clearly documented by Table 1 (which gathers electronic energies for TSs of propenol epoxidation). To confirm that the observed changes are in the correct direction, we carried out also single-point calculations with the large cc-pVTZ as well with the AUG-cc-pVTZ (which includes diffuse functions) basis set.[26] Inspection of Table 1 shows that the relative TS energies obtained with the AUG-cc-pVTZ basis set are similar to those from calculation with the 6-311+G** basis set, even if the latter basis set slightly favors the exo-TSs with respect to the former basis set.

As for the epoxidations of **5** and **6**, here we will report B3LYP/6-31G* fully optimized geometries and related energies as well as B3LYP/6-311+G**//B3LYP/6-31G* energies.[26]

All calculations were performed with the Gaussian 94[27] and Gaussian 98[28] suites of programs. All critical points have been characterized by diagonalizing the Hessian matrixes calculated for the optimized structures. Energies and geometrical data of conformational minima of 3-methyl-3-buten-2-ol (**5a**−**d**) and (*Z*)-3-penten-2-ol (**6a**−**d**) are reported in Table 2 (see also Figure 3). Transition structures have only one negative eigenvalue (first-order saddle points) with the corresponding eigenvector involving the expected formation of the two new oxirane bonds, the cleavage of the O_5-O_6, the lengthening of the $C_7=O_8$ and the shortening of the O_6-C_7 peroxy acid bonds (see **F** in Scheme 2 for TS numbering). The transition mode imaginary frequencies (cm^{-1}) of the TSs are reported (as ν_i) in Tables 3 and 4. The search for TSs was limited to concerted transition structures; i.e., only restricted B3LYP methods have been used.

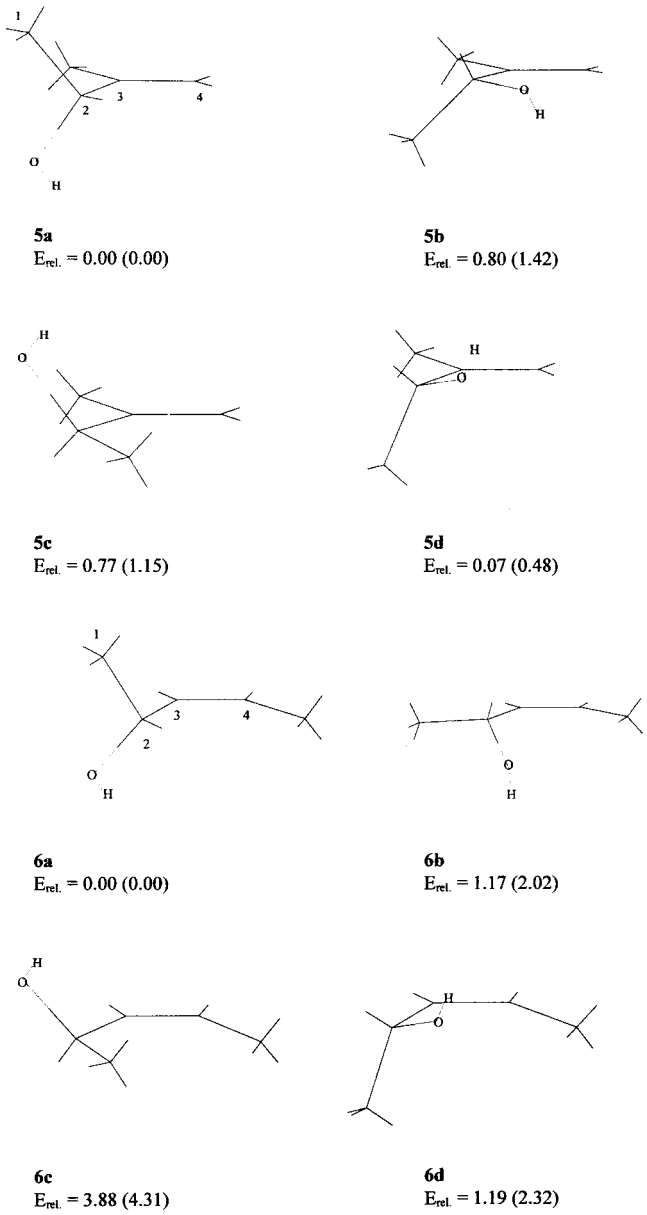

Figure 3. B3LYP conformational minima of 3-methyl-3-buten-2-ol (**5a**−**d**), (*Z*)-3-penten 2-ol (**6a**−**d**), and their relative energies (kcal/mol) at the B3LYP/6-31G* (B3LYP/6-311+G**//B3LYP/6-31G*) level.

Forming bond lengths are reported in Figures 4 and 5 while, in addition to α, β and β' angles (**F**, Scheme 2), the following angles are gathered in Tables 3 and 4: (i) the torsional angles ($H-O-C_2-C_3$ and $O-C_2-C_3-C_4$) necessary to describe rotations about the $O-C_2$ and C_2-C_3 bonds; (ii) the $X-O_5-O_6$ angle, which allows one to evaluate the alignment of the axis of the π cloud with the breaking O_5-O_6 bond (X is a dummy atom placed at the center of the C_3-C_4 bond, see **F** in Scheme 2); all calculated values are very close to 180°; (iii) the $H_9-O_5-O_6-C_7$ and $O_5-O_6-C_7-O_8$ torsional angles related to out-

(26) The cc-pVTZ basis sets have been suggested by a reviewer to be "proper" for hydrogen bonding description. However, they are highly time-consuming, specially after inclusion of diffuse functions, and out of reach, at least for us, for relatively large systems such as those studied in this work. For this reason, we used the B3LYP/6-311+G** level for single-point calculations on B3LYP/6-31G* geometries as an acceptable compromise between reliability and time request. However, the reader should keep in mind that this basis set might slightly overestimate (see Table 1) the stability of exo-TS (with hydrogen bonding to peroxy oxygens) as compared to that of their endo counterpart (with hydrogen bonding to carbonyl oxygen).

(27) Gaussian 94: Frisch, M. J.; Trucks, G. W.; Schlegel, H. B.; Gll, P. M. W.; Johnson, B. G.; Robb, M. A.; Cheeseman, J. R.; Keith, T.; Peterson, G. A.; Montgomery, J. A.; Raghavachari, K.; Al-Laham, M. A.; Zakrzewski, V. G.; Ortiz, J. V.; Foresman, J. B.; Cioslowski, J.; Stefanov, B. B.; Nanayakkara, A.; Challacombe, M.; Peng, C. Y.; Ayala, P. Y.; Chen, W.; Wong, M. W.; Andres, J. L.; Replogle, E. S.; Gompert, R.; Martin, R. L.; Fox, D. J.; Binkley, J. S.; Defrees, D. J.; Baker, J.; Stewart, J. P.; Head-Gordon, M.; Gonzales C.; Pople, J. A. Gaussian, Inc., Pittsburgh, PA, 1995.

(28) Gaussian 98, Revision A.6: Frisch, M. J.; Trucks, G. W.; Schlegel, H. B.; Scuseria, G. E.; Robb, M. A.; Cheeseman, J. R.; Zakrzewski, V. G.; Montgomery, J. A., Jr.; Stratmann, R. E.; Burant, J. C.; Dapprich, S.; Millam, J. M.; Daniels, A. D.; Kudin, K. N.; Strain, M. C.; Farkas, O.; Tomasi, J.; Barone, V.; Cossi, M.; Cammi, R.; Mennucci, B.; Pomelli, C.; Adamo, C.; Clifford, S.; Ochterski, J.; Petersson, G. A.; Ayala, P. Y.; Cui, Q.; Morokuma, K.; Malick, D. K.; Rabuck, A. D.; Raghavachari, K.; Foresman, J. B.; Cioslowski, J.; Ortiz, J. V.; Stefanov, B. B.; Liu, G.; Liashenko, A.; Piskorz, P.; Komaromi, I.; Gomperts, R.; Martin, R. L.; Fox, D. J.; Keith, T.; Al-Laham, M. A.; Peng, C. Y.; Nanayakkara, A.; Gonzalez, C.; Challacombe, M.; Gill, P. M. W.; Johnson, B.; Chen, W.; Wong, M. W.; Andres, J. L.; Gonzalez, C.; Head-Gordon, M.; Replogle, E. S.; Pople, J. A. Gaussian, Inc., Pittsburgh, PA, 1998.

Table 3. Bond Lengths (Å), Angles (Deg), Transition Mode (ν_i), OH Stretching Frequency (ν_{OH}), and Dipole Moment (μ) for the TSs of the PFA Epoxidation of 5 at the B3LYP/6-31G* Level[a,b]

parameter[c]	*syn,endo, threo-* **13a**	*syn,endo, threo-* **14b**	*syn,exo, threo-* **15a**	*syn,exo, threo-* **16b**	*syn,endo, threo-* **17a**	*anti,exo, threo-* **18c**	*syn,endo, erythro-* **19c**	*syn,endo, erythro-* **20d**	*syn,exo, erythro-* **21c**	*syn,exo, erythro-* **22d**	*syn,endo, erythro-* **23c**	*anti,exo, erythro-* **24a**
C_3-C_4	1.370	1.368	1.372	1.372	1.374	1.374	1.372	1.370	1.374	1.372	1.374	1.374
O_6-C_7	1.288	1.289	1.293	1.293	1.290	1.290	1.287	1.289	1.293	1.293	1.289	1.291
C_7-O_8	1.240	1.238	1.235	1.234	1.237	1.236	1.239	1.237	1.234	1.234	1.238	1.236
$H-O-C_2-C_3$	73.7	−89.7	55.3	−62.4	51.0	−73.9	−73.2	89.5	−55.8	54.2	−51.4	65.7
$O-C_2-C_3-C_4$	−131.1	−15.4	−124.6	−12.78	−131.93	114.9	127.8	21.3	122.6	20.8	131.2	−110.8
$X-O_5-O_6$	170.5	171.6	174.3	175.4	173.8	176.5	170.9	171.1	174.7	175.7	173.6	176.1
$H_9-O_5-O_6-C_7$	17.2	13.1	0.4	1.3	0.3	0.2	14.8	18.4	0.8	0.8	0.0	0.6
$O_5-O_6-C_7-O_8$	3.7	2.2	0.2	0.2	1.2	0.2	3.3	4.3	0.3	0.2	0.7	0.4
$\lvert 180° - \alpha \rvert$	5.0	6.3	4.2	6.4	4.8	6.9	5.5	5.1	4.5	5.5	5.4	7.8
β	96.0	92.8	85.4	85.1	91.9	89.0	97.1	93.5	85.4	85.2	92.4	89.4
β'	89.0	93.6	98.8	101.2	93.0	97.9	88.4	91.7	98.0	99.7	92.9	98.4
γ	56.6	78.6	87.7	74.9	115.5	86.1	56.1	73.5	88.6	71.7	121.7	81.2
δ	88.4	89.4	87.8	88.2	83.2	93.1	89.5	86.5	88.8	87.0	82.5	94.8
ν_i (cm^{-1})	399	401	396	401	395	426	407	398	398	404	394	427
ν_{OH} (cm^{-1})	3607	3620	3681	3690	3696	3717	3604	3595	3673	3683	3686	3729
μ (Debye)	2.93	2.91	3.45	2.99	3.63	3.60	2.97	3.10	3.40	3.34	3.51	3.46

[a] O_4-H_9 bond length in TS **13**−**23** is in the range 0.983−1.003 Å. [b] HCOOOH ground-state geometry: O_5-O_6, 1.444 Å; O_6-C_7, 1.343 Å; C_7-O_8, 1.209 Å; O_5-H_9, 0.989 Å; H−O−O−C and O−O−C−O = 0°; μ = 1.32 D. [c] For the numbering and the meaning of α, β, β' γ, and δ see **F** and **H** in Scheme 2.

Table 4. Bond Lengths (Å), Angles (Deg), Transition Mode (ν_i), OH Stretching Frequency (ν_{OH}), and Dipole Moment (μ) for the TSs of the PFA Epoxidation of 6 at the B3LYP/6-31G* Level

parameter	*syn,endo, threo-* **25a**	*syn,endo, threo-* **26b**	*syn,exo, threo-* **27a**	*syn,exo, threo-* **28b**	*syn,endo, erythro-* **29c**	*syn,endo, erythro-* **30d**	*syn,exo, erythro-* **31c**	*syn,exo, erythro-* **32d**
C_3-C_4	1.374	1.376	1.374	1.374	1.376	1.374	1.376	1.374
O_6-C_7	1.287	1.289	1.293	1.293	1.285	1.289	1.293	1.293
C_7-O_8	1.240	1.234	1.233	1.235	1.241	1.235	1.234	1.235
$H-O-C_2-C_3$	72.2	−87.6	53.2	−51.7	−72.1	80.9	−56.1	51.2
$O-C_2-C_3-C_4$	−136.3	−55.3	−135.3	−35.2	135.7	31.4	138.8	34.4
$X-O_5-O_6$	173.7	175.5	177.7	179.8	173.9	174.0	177.6	179.5
$H_9-O_5-O_6-C_7$	17.9	55.4	0.7	0.2	17.8	20.3	1.0	0.1
$O_5-O_6-C_7-O_8$	4.1	10.8	0.4	0.2	4.1	4.5	0.5	0.1
$\lvert 180° - \alpha \rvert$	5.5	6.2	4.9	5.9	5.5	6.2	5.0	5.9
β	99.9	97.3	89.8	90.9	100.3	98.6	89.6	89.8
β'	85.5	88.8	95.1	94.9	85.2	87.6	95.4	95.6
δ	85.0	84.4	83.3	87.8	85.4	80.3	82.4	88.1
γ	53.5	32.8	98.8	81.3	49.6	70.2	101.4	81.8
ν_i (cm^{-1})	392	408	387	389	393	387	390	389
ν_{OH} (cm^{-1})	3618	3555	3694	3688	3611	3592	3683	3698
μ (Debye)	3.66	4.00	3.81	2.74	3.71	2.69	3.77	2.92

of-plane distortion of the peroxy acid moiety; (iv) γ, the angle between the $O_5-O_6-C_7$ plane of the attacking peroxy acid and the $C_3{=}C_4$ bond axis; a value lower than 90° means that the C_7O_8 peroxy acid fragment is closer to C_3 than to C_4 (see **H**, Scheme 2) as a result of rotation around the O_5-O_6 bond; and (v) δ, the dihedral angle between the $O_5-O_6-C_7$ plane of the peroxy acid and the mean plane of the double bond moiety; a value larger (smaller) than 90° means that the peroxy acid plane is tilted away from (toward) the CMeHOH group.

A value of 90° for both γ and δ corresponds to a symmetrical spiro structure.[29]

Cartesian coordinates of reagents and all TSs are available on request.

To produce theoretical activation parameters at the B3LYP/6-31G* level, vibrational frequencies in the harmonic approximation were calculated for all the optimized structures and used, unscaled,[30] to compute the zero-point energies, their thermal corrections, the vibrational entropies, and their contributions to activation enthalpies, entropies, and free enthalpies (see left part of Tables 5 and 6). Moreover, electronic energies at the B3LYP/6-311+G** level were obtained by single point calculations on the fully optimized B3LYP/6-31G* geometries and used (with B3LYP/6-31G* molecular motion contribution and solvent effects) to evaluate free enthalpies both in the gas phase and in solution (right part of Tables 5 and 6).

The contribution of solvent effects to the activation free enthalpy of the reactions under study were calculated via the self-consistent reaction field (SCRF) method using the CPCM method (dichloromethane as solvent) as implemented in Gaussian 98 by single-point calculations (i.e., with unrelaxed gas-phase geometries of reactants and TSs) at the B3LYP/6-31G* level (Tables 5 and 6).[31]

Results

Conformers of 3-Methyl-3-buten-2-ol (5) and of (*Z*)-3-Penten-2-ol (6). We located four conformational

(29) It should be realized that the γ and δ angles practically also correspond to the angles between the mean PFA plane and, respectively, the $C_3{=}C_4$ bond axis and the $C_3{=}C_4$ plane in **15a**, **16b**, **17a**, **18c**, **21c**, **22d**, **23c**, **24a**, **27a**, **28b**, **31c**, and **32d** (all these TSs exhibit a planar PFA moiety). However, this is not true for TSs with out-of-plane distorted PFA moiety as in **13a**, **14b**, **19c**, **20d**, **25a**, **26b**, **29c**, and **30d** (in which both H_9 and O_8 are rotated out of the $O_5-O_6-C_7$ plane by ≥55° and ≥11°, respectively). This distortion obviously compounds the spiro/planar TS classification.

(30) Rastelli, A.; Bagatti, M.; Gandolfi, R. *J. Am. Chem. Soc.* **1995**, *117*, 4965.

(31) Solvent effects (both absolute and relative) evaluated by this method are smaller than those obtained with the Tomasi method (as implemented in Gaussian 94) previously used by us. Because the performance of methods in evaluating the solvent effects is not, to date, satisfactorily assessed the "computed solvent effect" should be taken with some caution.

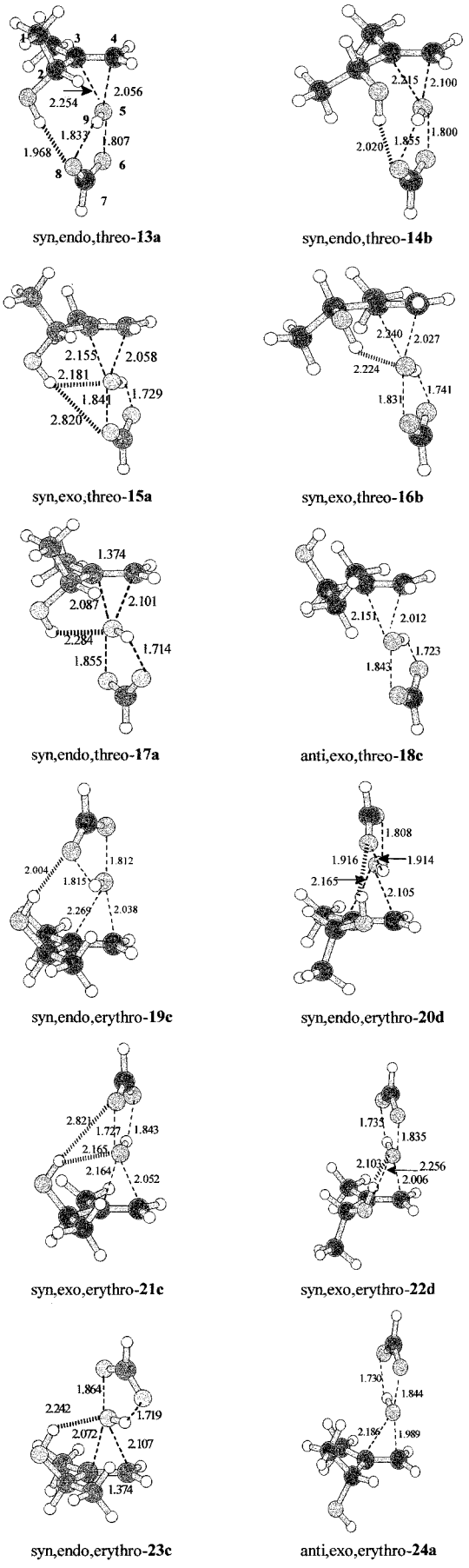

Figure 4. B3LYP/6-31G*-optimized transition structures (bond lengths in Å) for epoxidation of 3-methy-3-buten-2-ol (**5**) with peroxyformic acid.

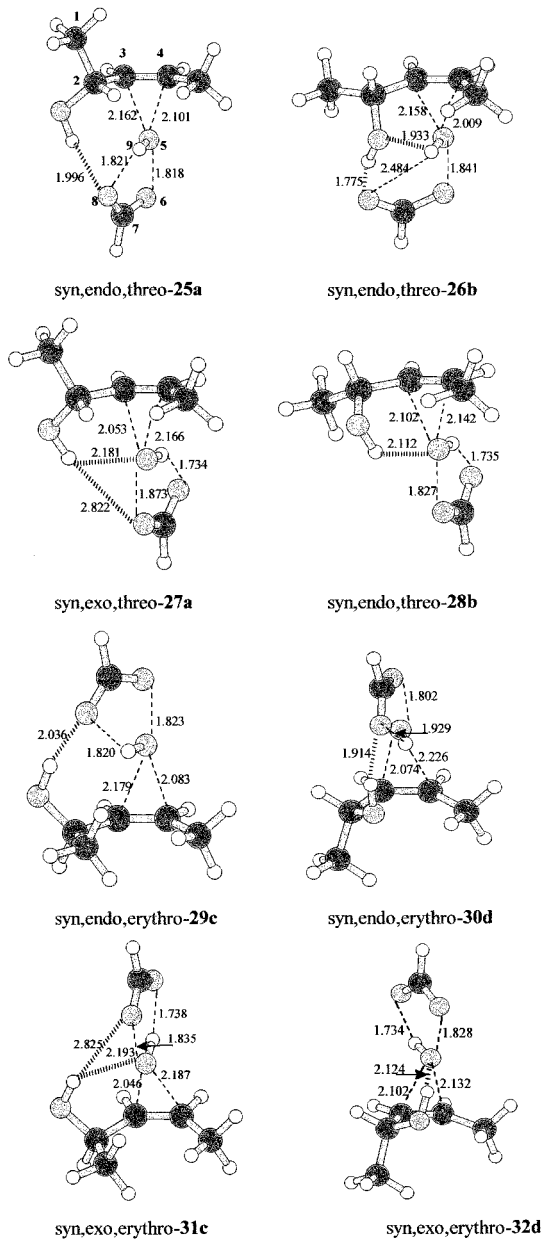

Figure 5. B3LYP/6-31G*-optimized transition structures (bond lengths in Å) for epoxidation of (Z)-3-penten-2-ol (**6**) with peroxyformic acid.

minima namely **a**−**d**, for both **5** and **6** (Figure 3 and Table 2), in which the hydroxylic hydrogen points toward the π bond giving rise to a weak OH−π interaction and being properly oriented to be involved in hydrogen bonding with the attacking peroxy acid. These conformers can be converted into each other by rotation around the C_2-C_3 bond.[32]

Two conformers (conformers **a** and **c**) for both **5** and **6** have the OH group outside (away from the C=C bond) while the other two (conformers **b** and **d**) feature an OH inside with the OH group faces the C=C bond.

As for 3-methyl-3-buten-2-ol **5**, both the outside conformers, **5a** and **5c**, have the torsional angle $OC_2C_3C_4$

(32) We did not try to locate the related conformational minima with the hydroxylic hydrogen pointing away from the π bond. Conformational analysis of 2-propenol clearly demonstrated that conformers of this type (without hydrogen bonding interactions and with repulsive closed shell interactions between lone pairs and the π bond) are definitely less stable than those in which hydrogen bonding operates.

Table 5. Relative Electronic Energies ($E^{\ddagger}_{rel}$), Enthalpies ($H^{\ddagger}_{rel}$), Entropies ($S^{\ddagger}_{rel}$), Free Enthalpies [$G^{\ddagger}_{rel}$ (gas phase), $G^{\ddagger}_{sol,rel}$ (solution)] of the TSs (13a−24a) for the Epoxidation of 3-Methyl-3-buten-2-ol with PFA at the Becke3-LYP Level with 6-31G* and 6-311+G Basis Set (Theoretical Yields (%) of *threo*-7 and *erythro*-8)**

	B3LYP/6-31G*					B3LYP/6-311+G**//B3LYP/6-31G*					
	E_{rel}	H_{rel}[a]	$S^{\ddagger}_{el}$[a]	G_{rel}[a]	$G_{sol,rel}$[c]	E_{rel}[d]	G_{rel}[d]	$G_{sol,rel}$[c,d]			
5a	0.00	0.00	0.00	0.00	0.00	0.00	0.00	0.00			
5b	0.80	0.75	−0.60	0.91	0.55	1.42	1.53	1.17			
5c	0.77	0.79	−0.23	0.85	0.63	1.15	1.23	1.01			
5d	0.07	0.02	−0.20	0.07	0.01	0.48	0.48	0.42			
	$E^{\ddagger}_{rel}$	$H^{\ddagger}_{rel}$[a]	$S^{\ddagger}_{rel}$a	$G^{\ddagger}_{rel}$[a]	yield, %[b]	$G^{\ddagger}_{sol,rel}$[c]	yield, %	$E^{\ddagger}_{rel}$[d]	$G^{\ddagger}_{rel}$[d]	yield, %	$G^{\ddagger}_{sol,rel}$[c,d]	yield, %
syn,endo,threo-**13a**	1.16	1.09	−0.95	1.34	5.0	1.38	3.7	0.67	0.85	3.2	0.89	1.5
syn,endo,threo-**14b**	0.81	0.86	−1.91	1.38	5.0	1.69	1.9	1.34	1.91	0.5	2.22	0.02
syn,exo,threo-**15a**	1.61	1.44	0.54	1.29	5.0	1.05	6.7	0.34	0.02	14.6	−0.22	11.8
syn,exo,threo-**16b**	2.29	2.07	1.37	1.70	2.5	1.35	3.7	1.39	0.80	3.5	0.45	3.3
syn,endo,threo-**17a**	3.14	2.84	1.24	2.50	0.5	2.03	1.0	1.99	1.35	1.2	0.88	1.6
anti,exo,threo-**18c**	6.18	5.90	2.66	5.18		3.35		4.16	3.16		1.33	0.6
threo-**7** (%)					**18**		**17**			**23**		**19**
syn,endo,erythro-**19c**	2.48	2.42	1.53	2.85		2.90		2.39	2.75	0.1	2.80	
syn,endo,erythro-**20d**	0.00	0.00	0.00	0.00	63.1	0.00	50.0	0.00	0.00	15.4	0.00	7.9
syn,exo,erythro-**21c**	2.48	2.31	−0.04	2.32	0.6	2.01	1.0	1.59	1.43	1.1	1.12	1.0
syn,exo,erythro-**22d**	1.57	1.35	2.49	0.67	18.3	0.23	32.0	0.16	−0.74	60.3	−1.18	70.4
syn,endo,erythro-**23c**	3.76	3.44	0.34	3.54		3.16		3.30	3.08		2.70	0.1
anti,exo,erytho-**24a**	5.59	5.33	2.58	4.63		2.83		3.62	2.66	0.1	0.86	1.6
erythro-**8** (%)					**82**		**83**			**77**		**81**

[a] Energies in kcal/mol and entropies in cal/mol K (eu); harmonic approximation assumed; standard state (273 K) of the molar concentration scale. B3LYP/6-31G* energies (E, hartree), thermal correction to enthalpy (δH, kcal/mol), entropy (S, eu) and thermal correction to free enthalpies (kcal/mol) for **5a**: $E = -271.749032$, $\delta H = 93.72$; $S = 80.53$, $\delta G = 71.73$. HCOOOH: $E = -264.879655$, $\delta H = 26.15$; $S = 64.08$, $\delta G = 8.64$. *syn,endo,erythro*-**20d**: $E^{\ddagger} = -536.618967$, $\delta H^{\ddagger} = 119.99$; $S^{\ddagger} = 104.34$, $\delta G^{\ddagger} = 91.49$; $\Delta E^{\ddagger} = 6.03$ kcal/mol; $\Delta G^{\ddagger} = 15.46$ kcal/mol; and $\Delta S^{\ddagger} = -31.91$ eu. [b] Yield (%) of the final diastereoisomer originating from each TS (**7** from threo TSs and, respectively, **8** from erythro TSs). [c] Solvent effects (kcal/mol) introduced by using the CPCM method (CH_2Cl_2 as solvent) at the B3LYP/6-31G* level: $\delta G_{sol} = G_{sol} - G_{gas}$: **5a** $\delta G_{sol} = -3.35$; HCOOOH $\delta G_{sol} = -3.28$; *syn,endo,erythro*-**20d** $\delta G^{\ddagger}_{sol} = -4.41$. [d] Energies (kcal/mol) have been obtained by B3LYP/6-311+G** single-point calculations on the fully optimized B3LYP/6-31G* geometries. For evaluation of the thermodynamic properties the B3LYP/6-31G* computed kinetic contributions are used. B3LYP/6-311+G** energies (hartree) **5a**: $E = -271.840550$; HCOOOH: $E = -264.972745$; *syn,endo,erythro*-**20d**: $E^{\ddagger} = -536.799103$; $\Delta E^{\ddagger} = 8.42$; $\Delta G^{\ddagger} = 17.85$ kcal/mol.

Table 6. Relative Electronic Energies ($E^{\ddagger}_{rel}$), Enthalpies ($H^{\ddagger}_{rel}$), Entropies ($S^{\ddagger}_{rel}$), Free Enthalpies [$G^{\ddagger}_{rel}$ (gas phase), $G^{\ddagger}_{sol,rel}$ (solution)], and Yield (%) of the TSs (25a−32d) for the Epoxidation of (*Z*)-3-Penten-2-ol with PFA at the Becke3-LYP Level with 6-31G* and 6-311+G Basis Set (Theoretical Yields (%) of *threo*-9 and *erythro*-10)**

	B3LYP/6-31G*					B3LYP/6-311+G**//B3LYP/6-31G*					
	E_{rel}	H_{rel}[a]	$S^{\ddagger}_{el}$[a]	G_{rel}[a]	$G_{sol,rel}$[c]	E_{rel}[d]	G_{rel}[d]	$G_{sol,rel}$[c,d]			
6a	0.00	0.00	0.00	0.00	0.00	0.00	0.00	0.00			
6b	1.17	1.09	0.29	1.01	1.50	2.02	1.86	2.35			
6c	3.88	4.08	−0.62	4.25	4.21	4.31	4.68	4.44			
6d	1.19	1.26	−0.91	1.51	1.64	2.32	2.64	2.77			
	$E^{\ddagger}_{rel}$	$H^{\ddagger}_{rel}$[a]	$S^{\ddagger}_{rel}$[a]	$G^{\ddagger}_{rel}$[a]	yield, %[b]	$G^{\ddagger}_{sol,rel}$[c]	yield, %	$E^{\ddagger}_{rel}$[d]	$G^{\ddagger}_{rel}$[d]	yield, %	$G^{\ddagger}_{sol,rel}$[c,d]	yield, %
syn,endo,threo-**25a**	1.28	1.14	1.47	0.75	2.7	0.98	1.9	−0.34	−0.87	0.6	−0.64	0.3
syn,endo,threo-**26b**	0.00	0.00	0.00	0.00	10.7	0.00	11.8	0.00	0.00	0.1	0.00	0.1
syn,exo,threo-**27a**	0.42	0.17	3.46	−0.77	44.6	−0.91	63.6	−2.38	−3.57	88.4	−3.71	93.5
syn,exo,threo-**28b**	1.06	0.73	3.61	−0.25	17.0	0.11	9.7	−0.70	−2.01	4.9	−1.65	2.1
threo-**9** (%)					**75**		**87**			**94**		**96**
syn,endo,erythro-**29c**	5.19	5.28	0.25	5.22		5.53		4.06	4.09	−	4.40	
syn,endo,erythro-**30d**	0.13	0.20	1.53	−0.22	16.0	0.66	3.4	−0.38	−0.73	0.5	0.15	0.1
syn,exo,erythro-**31c**	4.10	4.03	2.82	3.27		3.24		1.74	0.91	−	0.88	
syn,exo,erythro-**32d**	1.14	0.93	3.08	0.09	9.0	0.12	9.6	−0.99	−2.04	5.5	−2.01	3.9
erythro-**10** (%)					**25**		**13**			**6**		**4**

[a] Energies in kcal/mol and entropies in cal/mol K (eu); harmonic approximation assumed; standard state (273 K) of the molar concentration scale. B3LYP/6-31G* energies (E, hartree), thermal correction to enthalpy (δH, kcal/mol), entropy (S, eu) and thermal correction to Gibbs free energy (kcal/mol) **6a**: $E = -271.747155$, $\delta H = 93.83$; $S = 82.26.$, $\delta G = 71.36$. HCOOOH: $E = -264.879655$, $\delta H = 26.15$; $S = 64.08$, $\delta G = 8.64$. *syn,endo,erythro*-**26b**: $E^{\ddagger} = -536.616000$, $\delta H^{\ddagger} = 120.16$; $S^{\ddagger} = 102.75$, $\delta G^{\ddagger} = 92.09$; $\Delta E^{\ddagger} = 5.61$ kcal/mol; $\Delta G^{\ddagger} = 16.17$ kcal/mol and $\Delta S^{\ddagger} = -35.72$ eu. [b] Yield (%) of the final diastereoisomer originating from each TS (**9** from threo TSs and, respectively, **10** from erythro TSs). [c] Electrostatic solvent effect (kcal/mol) is introduced by using the CPCM method (CH_2Cl_2 as solvent) at the B3LYP/6-31G* level. $\delta G_{sol} = G_{sol} - G_{gas}$: **6a** $\delta G_{sol} = -4.20$; HCOOOH $\delta G_{sol} = -3.28$; *syn,endo,erythro*-**26b** $\delta G^{\ddagger}_{sol} = -5.59$. [d] Energies (kcal/mol) have been obtained by B3LYP/6-311+G** single-point calculations on the fully optimized B3LYP/6-31G* geometries. For evaluation of the thermodynamic properties the B3LYP/6-31G* computed kinetic contributions are used. B3LYP/6-311+G** energies (hartree) **6a**: $E = -271.839427$; HCOOOH: $E = -264.972745$; *syn,endo,erythro*-**26b**: $E^{\ddagger} = -536.794567$; $\Delta E^{\ddagger} = 9.03$ kcal/mol, $\Delta G^{\ddagger} = 19.59$ kcal/mol.

very close to |120°|. Conformer **5a** is more stable than **5c** probably as a result of higher ^{1,3}A strain in the latter as compared to the ^{1,2}A strain in the former. In the inside conformers **5b** and **5d** the O−C_2 bond is only slightly rotated down (by −3°) and up (by 16°), respectively, with respect to the C=C plane. The stronger ^{1,2}A strain in **5b** than in **5d** certainly dictates the higher stability of the latter as compared to the former.

In the case of (*Z*)-3-penten-2-ol, the outside conformer **6a** has the torsional angle $OC_2C_3C_4$ close to −120°,

Scheme 2

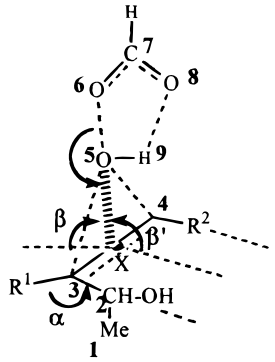

F (TS model, showing α, β, β' and XO_5O_6 angles and the numbering used for all TSs)

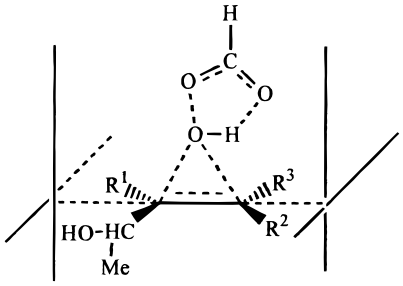

G (planar TS)

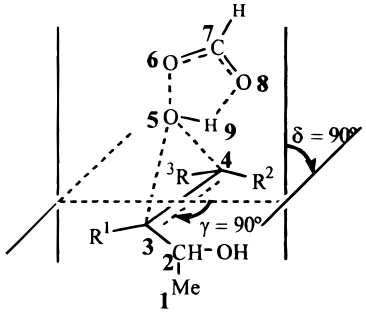

H (endo spiro TS)

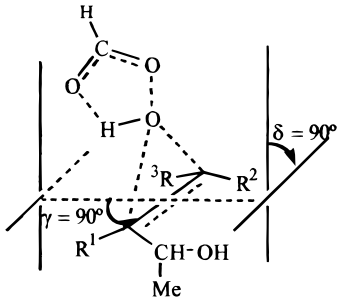

I (exo spiroTS)

whereas a counterclokwise rotation around the C_2-C_3 bond, to accommodate steric repulsion between the two methyl groups, widens this angle to 130° in the other outside conformer **6c**. The strong ^{1,3}A strain makes conformer **6c** much less stable than **6a** and also definitely less stable than both the inside conformers **6b** and **6d**. In the inside conformers **6b** and **6d** the $O-C_2$ bond is substantially rotated out of double bond plane down (by −48°) and, respectively, up (by 29°) here again to lessen ^{1,3}A strain (steric congestion between the OH and the methyl group on the double bond).

On going from reactants to TSs, conformers **5a**−**d** as well as **6a**−**d** experience some conformational change as a result of rotation around the C_2-C_3 and C_2-O bonds in order to maximize hydrogen bonding (in syn attacks) and/or to better accommodate steric repulsions (in particular ^{1,2}A and ^{1,3}A strains). However, we will see that each TS looks as it was strictly related to only one of the conformers.[33]

Thus, one can try to make previsions about face selectivity of epoxidation reactions on the basis of alcohol ground-state structures assuming that (i) factors that govern the conformer relative energies (A strains) are to a large extent maintained in related TSs and (ii) reaction pathways favored by hydrogen bonding dominate.

Geometries and energies of conformers **5a**−**d** suggest that bottom attack on outside **5a** and top attack on inside **5d** should be the most appealing pathways (competing each other in a balanced way) for producing threo **7** and erythro **8**, respectively. However, one can anticipate that also bottom attack on **5b** and top attack on **5c** can to some extent contribute to formation of threo **7** and erythro **8**, respectively. All these approaches can obviously take advantage from hydrogen bonding interaction between the reacting partners.

threo-**9** and *erythro*-**10** epoxides from alcohol **6** should derive mostly from the peroxy acid approach to the bottom face of outside **6a** and to the top face of inside **6d**, respectively, however with the threo pathway largely prevalent over the erythro one.

Thus, qualitative predictions based on alcohols structures seem to assign a prevalent role to inside conformers in formation of erythro epoxides and to outside conformers in formation of their threo counterparts.

Transition Structures for the Reactions of 5 and 6 with PFA: Geometries and the Planar vs Spiro Problem. The attack by peroxyformic acid on the conformers of **5** and **6** can take place syn or anti with respect to the OH group giving rise to syn and anti TSs. We have focused our study on syn TSs that benefit from hydrogen bonding, and only two anti TSs were located, for the sake of comparison, for the epoxidation of **5**.

As for the peroxy acid plane, it can adopt two perfectly planar ($\gamma = 0°$ and 180°, $\delta = 90°$) orientations (one, i.e., **G**, is depicted in Scheme 2) and two perfectly spiro ($\gamma = 90°$, $\delta = 90°$) orientations, namely the endo (the $C_7O_8H_9$ peroxy acid moiety on the same side of the MeCHOH substituent, **H** in Scheme 2) and exo (**I** in Scheme 2) ones. Conformations with γ values in the range $0° < \gamma < 180°$

(33) Obviously our system behaves as a Curtin−Hammett system. The conformational equilibrium of the starting alcohols is very fast and product distribution is only determined by the relative TS energies. Thus, to calculate theoretical face selectivity one does not need to know which conformer each TS originates from.

are obviously accessible to the peroxy acid moiety. TSs with γ in the range 60°−120° can be classified as spiro while those with γ in the range 0°−30° or 150°−180° as planar-like. With the exception of the two planar structures all other TSs, with $\gamma \neq 0°$ or 180°, can have either an endo or exo orientation.

In some cases, such as for syn,endo TSs, the problem of planar/spiro classification is compounded and made less definite by the non planarity of the peroxy acid moiety owing, in particular, to the noticeable distortion of the hydrogen atom out of the heavy atom plane.

Finally, attacks on the bottom face and on the top face of conformers **5a**−**d** and **6a**−**d** afford, respectively, the threo and the erythro epoxide.

TSs will be given descriptors that indicate all the above characteristics: e.g., *syn*,*endo*,*threo*-**a** indicates a TS formally deriving from a syn endo attack by PFA on the bottom face of the conformer **a**.

The first-order saddle points **13**−**32** (18 syn and two anti) located for the reaction of PFA with both **5** and **6** are reported in Figures 4 and 5.

Inspection of geometry data (Tables 3 and 4) shows that on passing from the starting alcohols to the corresponding TSs rotation of the $O-C_2$ bond around the C_2-C_3 bond, although not negligible, is far from being dramatic (it is less than 13° and in several cases less than 10°). That is, the alcohol moiety substantially retains in the TSs the conformation of the starting molecule. Consenquently, ^{1,2}A and ^{1,3}A strains are likely to operate in a similar way in dictating the relative energies of the starting conformers and of the corresponding TSs.

Only the O−H bond in *syn*,*endo*,*threo*-**26b** and *syn*,*endo*,*erythro*-**30d** heavily rotates (by ∼40°) around the $O-C_2$ bond to adjust its position for a better hydrogen bonding interaction with the PFA carbonyl oxygen.

The peroxy acid moiety maintains its ground-state planar array of atoms in all TSs with hydrogen bond to peroxy oxygens (i.e., $O_5O_6C_7O_8$ and $H_9O_5O_6C_7 \leq 1°$ in all syn,exo TSs as well as in syn,endo TSs **17a** and **23**c and anti TSs). In contrast, a noticeable out-of-plane distortion is present in syn,endo TSs with hydrogen bond to carbonyl oxygen (**13a**, **14b**, **19c**, **20d**, **25a**, **26b**, **29c**, and **30d**), as documented by the $O_5O_6C_7O_8$ (2°−11°) and $H_9O_5O_6C_7$ (13°−55°) dihedral angles. This distortion is the result of a large rotation of the O_5-H_9 bond and of a small one of $C_7=O_8$ bond around the breaking $O_5\cdots O_6$ bond away and, respectively, toward the OH group on the olefin.

TSs **13**−**32** exhibit, in addition to the above-described geometry features, several other structural details already present in TSs **1a**−**4b** for the reaction of PFA with propenol. In short: (i) asynchronicity in C···O bond fomation is low; (ii) out-of-plane deformation of the alkene fragment (α) and elongation of the C=C bond are small; (iii) there is a slight inclination of the forming oxirane plane (as a rule, $\beta > \beta'$ for endo TSs while $\beta' > \beta$ for exo TSs) to the opposite side of the C=O−H peroxy acid moiety; (iv) alignment of π bond axis with the breaking $O_5\cdots O_6$ is very good ($XO_5O_6 \geq 170°$) indicating a S_N2-like reaction; and (v) electron transfer from olefin to peroxy acid is sizable (∼0.3 electrons). *The largest net negative charge is located on the carbonyl oxygen (*∼*−0.6)* while that on the distal oxygen (O_6, ∼−0.4) is larger than that on the proximal one (O_5, ∼−0.3; O_5H_9 as a whole, ∼0.04).[34]

In all syn,exo TSs, the OH group hydrogen bonds the PFA peroxy oxygens while in syn,endo TSs the PFA carbonyl oxygen acts, as a rule, as the hydrogen bond acceptor. However, for the epoxidation of **5** we have also located two syn,endo TSs, namely *syn*,*endo*,*threo*-**17a** (γ = 115.5) and *syn*,*endo*,*erythro*-**23c** (γ = 121.7), in which hydrogen bonding involves the PFA peroxy oxygens.

Hydrogen bonding to the carbonyl oxygen (which has the highest negative net atomic charge) in syn,endo TSs is stronger than hydrogen bonding interactions to peroxy oxygens in the corresponding syn,exo TSs. In fact, ν_{OH} in the former TSs is ≥60 cm^{-1} lower than that in the latter ones (see Tables 3 and 4). The resulting energetic stabilization of syn,endo with respect to syn,exo TSs is counteracted by adverse entropy effects, a sizable out of plane distortion of the peroxy acid moiety and a higher steric congestion.

In syn,exo TSs with OH in the inside position (**16b**, **22d**, **28b**, and **32d**) hydrogen bonding involves the proximal peroxy oxygen (O_5) while the whole peroxy system ($O_5\cdots O_6$) can be considered engaged in this interaction when OH adopts the outside conformation (*syn*,*exo*-**15a**, **21c**, **27a**, and **31c**).

Therefore, what about the spiro vs planar (Henbest−Adam model) TS geometry?

All of the TSs for the reactions of **5** and **6** show some distortions with respect to an ideal spiro (i.e., with a planar peroxy acid moiety oriented at 90° to the $C_3=C_4$ bond axis, i.e., $O_5O_6C_7O_8 = H_9O_5O_6C_7 = 0°$ and $\gamma = \delta = 90°$) orientation. For example, γ (the angle between the $O_5\cdots O_6-C_7$ peroxy acid plane and the C_3-C_4 bond axis) varies in the range 56°−122° for TSs of 3-methyl-3-buten-2-ol (**5**) epoxidations and from 33° to 101° for TSs of (*Z*)-3-penten-2-ol (**6**) epoxidations. The γ values closest to 90° are shown by syn,exo TSs in which the OH group hydrogen bonds the peroxy oxygens while the peroxy acid moiety is almost planar.

Interesting is the geometry of two syn,endo TSs, that is, *threo*-**17a** and *erythro*-**23c**. In these TSs, the planar peroxy acid moiety is forced to a relatively large (by 25° and 32°, respectively) rotation away from perpendicularity, to the C=C bond axis, to properly orient the peroxy group for a good hydrogen bonding interaction with OH.

The largest deviations of the γ angle from 90° are found in syn,endo TSs in which the peroxy acid carbonyl oxygen is involved in hydrogen bonding and the peroxy acid moiety is strongly distorted out of planarity owing, in particular, to distortion of H_9 out of the PFA heavy atom plane. In this context, it is worthy to underline that the torsional angle $H_9O_5XC_3$ is close to 90° not only in syn,-exo but also in syn,endo TSs (it spans the range 67°−96°).[35] That is, the H_9O_5 bond is far from being parallel ($H_9O_5XC_3 = 0°$ or 180°) or nearly parallel to the $C_3=C_4$ bond axis as required by planar or planar-like geometries[13g] while it is closer to being orthogonal to this bond as required by the spiro geometry. The underlying reason for the latter observation is that the oxygen being transferred prefers a tetrahedral like over a square-planar like bonding geometry.

(34) For example, CHelpG net atomic charges for *syn*,*exo*,*threo*-**15a** (*syn*,*exo*,*erythro*-**22d**) are as follows: $O_5 = -0.31$ (0.34), $O_6 = -0.41$ (−0.39), $O_8 = -0.56$ (−0.56), O_5H_9 as a whole = +0.07 (+0.04). Electron transfer, from olefin to PFA, according to CHelpG analisys is −0.29 and −0.31 in *syn*,*exo*,*threo*-**15a** and *syn*,*exo*,*erythro*-**22d**, respectively.

(35) In other words, the $H_9O_5O_6$ peroxy acid plane is always very close to being orthogonal to C=C bond.

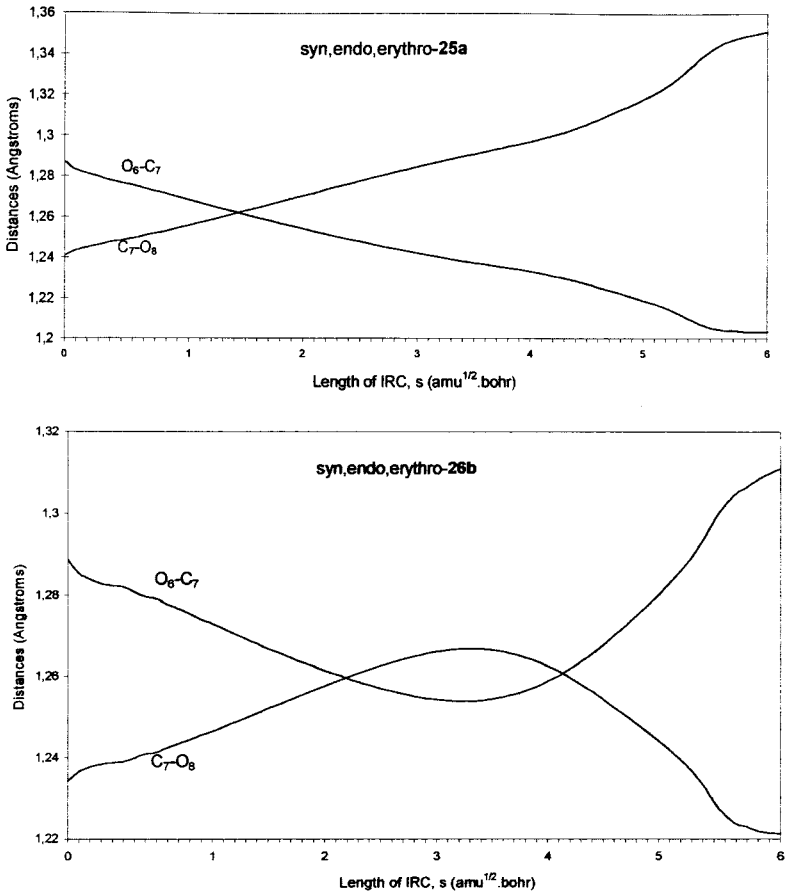

Figure 6. Change of internal coordinates along the IRC path from *syn,endo,erythro*-**25a** and *syn,endo,erythro*-**26b** to final products. The length of the IRC is given by s (amu$^{1/2}$ bohr) where $s = 0$ represents the transition structure and $s \rightarrow \infty$ the products.

These data provide compelling evidence that TS geometries for epoxidations of allylic alcohols with allylic strain substantially conform to a spiro butterfly orientation of the reactants. It is also quite clear that these TSs do not resemble the planar butterfly TS geometry ($\gamma = 0°$) of the Henbest−Adam model. However, passing from the ethylene reaction TS ($\gamma = 90°$) to TSs for the allylic alcohol reactions, significant rotations of the planar peroxy acid moiety around the $O_5\cdots O_6$ axis by $<30°$ (in both directions) can take place at a relatively low energy cost in syn,exo TSs and two syn,endo TSs while larger rotations are accompanied by strong out of plane distortions of the peroxy acid in most of syn,endo TSs. *We can conclude that the presence of a hydrogen-bonding interaction has a noticeable influence on TS geometry and in particular makes the peroxy acid moiety deviate from a perpendicular orientation with respect to C═C bond axis but it never does succeed in switching transition structures from spiro to planar geometries.*

It does not seem reasonable to expect that gas-phase higher level calculations (nor, we feel condensed-phase optimizations) can arrive at different conclusions as far as the spiro/planar problem is concerned. As emphasized above, we have shown that, for the propenol epoxidation, improving the basis set does not appreciably change TS geometries in particular those where hydrogen bonding is at work.

A New Mechanism for the Peroxy Acid Hydrogen Transfer: 1,2- as a Possible Alternative to 1,4-Hydrogen Transfer. It is well-known that the peroxy acid O−H bond length keeps on being almost unchanged on going from reactants to TSs (O_5-H_9 = 0.989 Å in HCOOOH and 0.983−1.003 Å in **13**−**32**) and animation of the imaginary frequency in TSs showed that there is practically no motion of H_9. The peroxy acid hydrogen (H_9) migration must occur after the barrier is crossed, and it has always been assumed that a 1,4-hydrogen shift, from the peroxy oxygen (O_5) to the former carbonyl oxygen (O_8), takes place. This hypothesis is the only reasonable one when the strong intramolecular hydrogen bonding ($H_9\cdots O_8$) in the planar peroxy acid moiety is maintained in the TS as, for example, in all syn,exo TSs.

However, in most endo TSs there is an out of plane distortion of the peroxy acid moiety as a result of replacement (at least in part) of the intramolecular, here $H_9\cdots O_8$, by the intermolecular ($OH\cdots O_8$) hydrogen bonding. It should be also underlined that, as shown by Bach et al.,[17] the hydrogen peroxy acid migration takes place when the $O_5\cdots O_6$ breakdown is well advanced so that it schematically can be depicted as involving a system constituted of a protonated epoxide ($O-H^+$) and a formiate anion. This is to say that in addition to the 1,4-hydrogen shift also an 1,2-hydrogen shift (from O_5 to O_6) may become a viable process.

We have carried out an IRC analysis from *syn,endo,threo*-**25a** and *syn,endo,threo*-**26b**, respectively, toward the final threo epoxide **9** (Figure 6 and Scheme 3). In the former case, there is a nice parallelism between lengthening of the C_7-O_8 bond and shortening of the O_6-C_7 bond while the $O_5\cdots O_6$ bond is progressively breaking down. The 1,4-hydrogen shift takes place only when the whole process is well advanced to give epoxide **9** and

Scheme 3

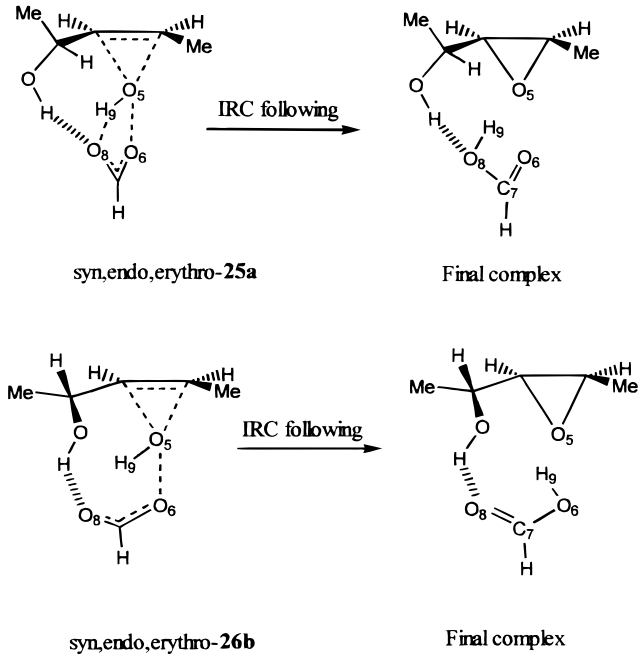

performic acid (Scheme 3). All this has already been described also by Bach et al. for the analogous TS of the propenol epoxidation (our *syn,endo*-**2b**, Figure 2).[17]

Things are different in the case of *syn,endo,threo*-**26b**, which shows by far the highest peroxy acid moiety distortion ($H_9O_5O_6C_7 = 55°$) owing to the almost complete replacement of the intramolecular hydrogen bonding with a strong ($\nu_{OH} = 3855$ cm^{-1} is the lowest observed among ν_{OH} for the olefinic OH group) intermolecular interaction ($O_8\cdots H_9 = 2.48$ Å vs $O_8\cdots HO = 1.78$ Å in **26b**). IRC following shows that immediately after the TS once again there is a lengthening of the C_7-O_8 bond accompanied by a shortening of the O_6-C_7 bond but, at $s \approx 3$, these processes are reversed (Figure 6). The C_7-O_8 bond begins to shorten and the O_6-C_7 bond to lengthen so that a crossing is observed ($s \approx 4.1$) in the diagram that represents these two internal coordinates as a function of the IRC length. The inversion and crossing points occur when the O_5-O_6 bond is stretched at 2.29 and 2.35 Å, respectively.

The 1,2-hydrogen shift (from O_5 to O_6) leads to a final complex where the formic acid carbonyl oxygen (and not the formic acid OH oxygen as in the case of syn,endo,-threo-**25a**) plays the role of hydrogen bond acceptor. In both mechanisms, the $O_8\cdots HO$ hydrogen bonding interaction is maintained throughout the whole process.

It is evident that the 1,2-hydrogen shift occurs for a TS with a quite particular geometry and it may well represent a relatively rare exception more than a general process always in competition with the 1,4-hydrogen migration.

Theoretical Diastereoselectivity: Epoxidation of 5. To discuss the stereoselectivity of epoxidation of **5** we are faced with 10 first order saddle points if we consider only TSs that feature a syn attack (with respect to the OH group) on the four conformers of **5** (Figure 3). In five of them the PFA attack occurs on the alcohol bottom face leading to the threo epoxide **7**, while in the other five TSs the PFA approach takes place on the alcohol top face affording the erythro isomer **8**. Moreover, the allylic OH adopts an outside and, respectively, inside conformation in six and four of them.

Thus, the stereoselectivity problem is much more complicated than Adam assumed it to be.[13] To compare our results with Adam's qualitative models we now address the important question of which are the TSs dictating the threo/erythro ratio and in particular which TS dominates (if there is one) in formation of the threo and, respectively, erythro epoxide.

As for the threo TSs, relative free enthalpies ($G^{\ddagger}_{rel}$) at the higher theory level (B3LYP/6-311+G**//B3LYP/6-31G*) (Table 5) demonstrate that *syn,exo,threo*-**15a** is the most stable TS both in gas phase (by ≥0.78 kcal/mol) and in dichloromethane solution (by ≥0.67 kcal/mol). *It is worth noting that this TS has the OH group in the outside position and hydrogen bonding to PFA peroxy oxygens. It conforms to qualitative predictions based on conformer ground state geometries and energies and substantially resembles, but with spiro geometry, the Adam's threo TS* (of the type **11**, Scheme 1). However, both in gas phase and in solution reaction channels through *syn,exo,threo*-**16b** (with OH inside and hydrogen bonding to peroxy oxygen), *syn,endo,threo*-**13a** (OH outside and hydrogen bonding to carbonyl oxygen), and *syn,endo,threo*-**17a** (OH outside and hydrogen bonding to peroxy oxygens) cannot be completely neglected since they as a whole account for ∼34% of epoxide **7** formation.

The lower theory level, i.e., B3LYP/6-31G*, predicts that four TSs should compete each other in a balanced way to produce **7** both in gas phase and in solution.

It is very important to stress that (i) passing from electronic energies or enthalpies to free enthalpies, (ii) improving the theory level, and (iii) adding solvent effects slightly disfavor syn,endo TSs with hydrogen bonding to carbonyl oxygen with respect to the corresponding syn,-exo TSs with hydrogen bonding to peroxy oxygens. For example, *syn,exo,threo*-**15a** is predicted less stable by 0.45 kcal/mol than *syn,endo,threo*-**13a** according to $E^{\ddagger}_{rel}$ at the B3LYP/6-31G* level and more stable by 1.11 kcal/mol according to $G^{\ddagger}_{sol,rel}$ calculated by using the higher level $E^{\ddagger}_{rel}$ and adding solvent effect. If we trust higher level $G^{\ddagger}_{sol,rel}$ *we will have to conclude that syn,endo TSs, with OH that hydrogen bonds the PFA carbonyl oxygen play a minor role in formation of* ***7***. Moreover, *TSs* ***a*** *with OH outside clearly overcome TSs* ***b*** *with OH inside and predictions about their relative role in formation of* ***7*** *do not heavily depend on theory level or solvent effects.*

The first part of the latter observation has to be reversed in the case of erythro TSs. *At both theory levels, no matter whether gas phase or solution data are considered, TSs* ***d*** *with OH inside clearly prevail over TSs* ***c*** *with OH outside. This finding stands in sharp contrast with the Adam's hypothesis that indicates TS* ***12,*** *with OH outside, as the only relevant pathway to* ***8*** while confirming Pierre's suggestion (see the Introduction)[16] as well as qualitative predictions (see Conformers...) derived from conformer ground-state geometries and energies.

Here again, as for the endo-exo TS pairs leading to threo **7**, *syn,exo,erythro*-**22d** is predicted less stable (by 1.57 kcal/mol) than *syn,endo,erythro*-**20d** at the electronic energy level ($E^{\ddagger}_{rel}$) evaluated by the B3LYP/6-31G* method while the latter should prevail (by 1.18 kcal/mol) in solution ($G^{\ddagger}_{sol,rel}$ calculated by using $E^{\ddagger}_{rel}$ from the B3LYP/6-311+G**//B3LYP/6-31G* calculations). Actually, according to the latter higher theory level, *erythro*-**8** derives largely from *syn,exo,erythro*-**22d**.

We did not carry out a systematic search for anti TSs, i.e., TSs that cannot be assisted by hydrogen-bonding interactions. We located two anti,exo TSs leading to *threo*-**7** and to *erythro*-**8**, respectively. They cannot compete in the gas phase with the most stable syn TSs, but in solution the energy gap between anti and syn TSs is strongly reduced. However, these two reaction channels do not appreciably contribute to epoxide formation.

Finally, on the basis of the 12 TSs located by us, we have calculated the theoretical diastereoselectivity of the PFA epoxidation of **5**. The erythro epoxide **8** is predicted as dominant at both theory levels and both in gas phase and solution. The predicted threo/erythro ratios in dichloromethane solution (**7**/**8** = 17:83 and 19:81 at the B3LYP/6-31G* and B3LYP/6-311+G**//B3LYP/6-31G* level, respectively) is definitely lower than the experimental one (45:55). However, it can be considered satisfying that, for such a complex system, theory correctly predicts formation of a diastereoisomer mixture with dominance of the erythro epoxide even if stability of erythro TSs is slightly overestimated as compared to that of threo TSs.

Theoretical Diastereoselectivity: Epoxidation of 6. In the case of **6**, the diastereoselectivity problem looks simpler than for **5**. All the remarks and comments on theory level as well as solvent effects on TS relative energies for epoxidation of **5** fully hold also for epoxidation of **6** (Table 6) and the discussion can be limited to $G^{\ddagger}_{sol,rel}$ calculated by using $E^{\ddagger}_{rel}$ from the B3LYP/6-311+G**//B3LYP/6-31G* method. In fact, theory suggests that *threo*-**9** is formed only via *syn*,*exo*,*threo*-**27a** while *erythro*-**10** comes only from *syn*,*exo*,*erythro*-**32d** as these TSs are more stable than their competitors by ∼2.1 kcal/mol. The former TS exhibits an OH outside conformation while in the latter TS the OH group is located in the inside position and both are exo TSs with the peroxy oxygens acting as the hydrogen bond acceptors. Quantitative calculations confirm qualitative predictions (see Conformers...) about the prevalent role of OH-outside conformers in formation of threo derivatives and of OH-inside conformers in formation of erythro derivatives as well as about the highly preferred formation of threo **9**.

As for Adam's models,[13a,c−i] TS **11** looks like *syn*,*exo*-,*threo*-**27a** (which, however, has a spiro geometry) while TS **12** is similar to *syn*,*exo*,*erythro*-**31c**. The latter can hardly play a dominant role in formation of erythro **10** given that, at all calculation levels, it is less stable than *syn*,*endo*,*erythro*-**30d** and, even more, it is always much less stable (by ≥2.90 kcal/mol) than *syn*,*exo*,*erythro*-**32d**.

Theoretical diastereoselectivity predictions in solution (**9**/**10** = 96:4) substantially reproduce the experimental threo/erythro ratio (**9**/**10** = 95:5).

Conclusion

Calculations at the B3LYP/6-31G* and B3LYP/6-311+G**//B3LYP/6-31G* theory levels about the mechanism of epoxidation of chiral acyclic allylic alcohols (3-methyl-3-buten-2-ol and (*Z*)-3-penten-2-ol) lead to the following observations.

Hydrogen bonding is operative in syn TSs with the OH group acting as hydrogen bond donor while the carbonyl oxygen and the peroxy oxygens of the peroxy acid compete each other as hydrogen bond acceptor. Anti TSs do not significantly contribute to the reaction stereochemical outcomes.

Geometry of all TSs has to be classified as spiro butterfly, i.e., with the peroxy acid plane close to a perpendicular orientation to the C═C bond axis. This statement rigorously holds for all TSs with hydrogen bonding to the peroxy oxygens (both endo and exo) that have a planar peroxy acid moiety. Endo TSs with hydrogen bonding to the carbonyl oxygen experience a strong out of plane distortion of the peroxy acid moiety and this introduces some ambiguity in the classification. However, no TSs were located that can be classified as planar butterfly (i.e., with the peroxy acid plane oriented at ≤30° to the C═C bond axis).

Hydrogen bonding stabilizes syn TSs and influences their geometry; however, it never succeeds in imposing a planar butterfly structure.

Conformations with the OH group occupying either an outside or an inside position come into play in determining product formation.

Endo TSs, with hydrogen bonding to the carbonyl oxygen, can have similar or even lower potential energy than their exo counterparts, with hydrogen bonding to the peroxy oxygens, at the B3LYP/6-31G* level. Improving the theory level as well as introduction of entropy and solvent effects disfavor the former with respect to the latter so that the highest level calculations suggest that endo TSs give a minor contribution to product formation. However, as for endo-exo TS competition, the only possible definitive conclusion, to date, is that both exo and endo TS must be taken into account to properly discuss selectivity in epoxidation of acyclic alcohols. It should be emphasized that the relative energies of TSs are quite compressed so that their predicted relative role might well slightly change as a result of higher level calculation or of a more proper evaluation of solvent effect.

IRC following disclosed a new mechanism for peroxy acid hydrogen transfer, a 1,2-shift instead of the more general 1,4-shift. This pathway can be preferred in endo TSs with a strongly puckered peroxy acid moiety.

The above observations demonstrate that the models (planar-butterfly with OH in outside conformation) advanced by Adam are not supported by calculations even if they correctly predict the important role of TSs with hydrogen bonding involving the peroxy oxygens.[13a−g]

In conclusion, on the basis of this DFT study, we state that resemble qualitative models for these reactions can be based on TSs featuring syn,exo spiro geometries with hydrogen bonding to peroxy acid peroxy oxygens and with the OH group either in outside or inside position. Moreover, meaningful prediction of the highly preferred formation of one diastereoisomer can be made only when, as in the case of **6**, the presence of a largely prevalent starting conformer with a syn face free from steric encumbrance indicates a reaction pathway that completely outweighs its possible competitors. In others cases (see **5**) one can at most anticipate formation of a diastereoisomer mixture.

Acknowledgment. Financial support from MURST and CNR is gratefully acknowledged.

JO991530K